

**NUMERICAL SIMULATION OF SUPERCRITICAL  
FLOW AT ABRUPT EXPANSION STRUCTURE  
WITH HIGHER ORDER SCHEME**

**LIM JIA JUN**

**UNIVERSITI SAINS MALAYSIA  
2019**

**NUMERICAL SIMULATION OF SUPERCRITICAL  
FLOW AT ABRUPT EXPANSION STRUCTURE  
WITH HIGHER ORDER SCHEME**

**by**

**LIM JIA JUN**

**Thesis submitted in fulfilment of the requirements**

**for the degree of**

**Master of Science**

**May 2019**

## ACKNOWLEDGEMENT

I would like to express my deepest gratitude to all those who helped me in one way or another, be it during my research work or the writing of my dissertation. First, I would like to thank Dr. Puay How Tion, my supervisor, for his continuous guidance, encouragement and constructive suggestion throughout my whole research work. It would not be possible for me to complete my research work without his valuable suggestions. Then I would like to express my gratitude to Professor Dato<sup>c</sup> Dr. Aminuddin Ab. Ghani for his support and guidance throughout this study. It was a great experience in carrying out my research work under him since I gained a lot of valuable knowledge.

Secondly, I would like to thank my colleagues, Ms Tah Ai Sher, Ms Siti Rohaya Jokefli, Mr Mohammad Faiz Abdullah and Mr Moon Wei Chek for always sharing ideas with me and helping me whenever I needed help. Without their help, it would not be possible for me to complete my research work.

I would also like to express my sincere appreciation to Ms Azra Azreen Kamarjalman, Ms Junaidah Abdullah, Ms Kirushantini A/P Balakrishnan, Ms Lum Pei Teng, Ms Nor Ariza Azizan, Ms Siti Fairuz Juiani, Ir. Dr. Chang Chun Kiat, Mr Lai Chee Hui, Mr Mohd Afiq Harun, Mr Muhammad Fitri Mohd Akhir, Mr Muhammad Kashfy Zainalfikry and Mr Syafiq Shahrudin for their support and inspiration.

Last but not least, I would like to thank my parents, Mr Lim Kok Seong and Madam Ong Tee Gnoh as they are my inspiration and it is with their great support and continuous care in my life that has led me to become who I am today. To my brothers, Mr Lim Jia Yang and Mr Lim Jia Jian, thank you for the continuous support and encouragement throughout my study. I apologize to all whose names have been missed out but have also helped and supported me in various ways.

# TABLE OF CONTENTS

<b>ACKNOWLEDGEMENT</b>	<b>ii</b>
<b>TABLE OF CONTENTS</b>	<b>iii</b>
<b>LIST OF TABLES</b>	<b>vi</b>
<b>LIST OF FIGURES</b>	<b>vii</b>
<b>LIST OF SYMBOLS</b>	<b>xiv</b>
<b>ABSTRAK</b>	<b>xvi</b>
<b>ABSTRACT</b>	<b>xvii</b>
<b>CHAPTER ONE: INTRODUCTION</b>	<b>1</b>
1.1 Background	1
1.2 Problem Statement	3
1.3 Objective	4
1.4 Scope of Work	4
1.5 Organisation of the Thesis	5
<b>CHAPTER TWO: LITERATURE REVIEW</b>	<b>7</b>
2.1 Overview	7
2.2 State of Flow	7
2.3 Mechanics of Supercritical Flow	8
2.4 Expansion in Supercritical Flow	9
2.5 Abrupt Expansion Experimental Study	10
2.6 Flow Characteristics of Supercritical Flow at Abrupt Expansion Channel	10
2.7 Analytical Study	12

2.8	Constrained Interpolation Profile (CIP) Scheme	14
2.9	FLOW-3D model	14
2.10	Dam Break Flow Problem	15
2.11	Discrepancy Ratio	16
2.12	Summary	16
<b>CHAPTER THREE: METHODOLOGY</b>		<b>17</b>
3.1	Introduction	17
3.2	Development of Numerical Model (DA-CIP)	19
3.2.1	Numerical Algorithm (One-dimensional problem)	21
3.2.2	Numerical Algorithm (Two-dimensional Problem)	24
3.2.3	Verification of Numerical Model	28
3.3	Simulation of Supercritical Flow at Abrupt Expansion Channel	33
3.3.1	Verification of DA-CIP model against analytical solution	34
3.3.2	Validation of numerical model experimental results	35
3.4	FLOW-3D Model Development	36
3.4.1	Model Setup – Physics	37
3.4.2	Model Setup – Fluids	39
3.4.3	Model Setup – Meshing and Geometry	40
3.4.4	Model Setup – Boundary Conditions	46
3.4.5	Simulation Manager	47
3.5	Development of Physical Model	48
3.5.1	Test Channel Setting	49
3.5.2	Measuring Devices	52

3.5.3	Test Channel Modification	57
3.7	Summary	58
<b>CHAPTER FOUR: RESULTS AND DISCUSSION</b>		<b>59</b>
4.1	Introduction	59
4.2	Mesh Convergence Test for One-dimensional Dam Break Flow Problem	59
4.3	Verification of Numerical Model	61
	4.3.1 One-dimensional Dam Break Problem	61
	4.3.2 Two-Dimensional Partial Dam Break Problem	66
4.4	Verification of DA-CIP model against Analytical Solution of Abrupt Expansion Flow	69
4.5	Validation between DA-CIP model against Experimental Results	79
4.6	Summary	104
<b>CHAPTER FIVE: CONCLUSION AND RECOMMENDATION</b>		<b>105</b>
5.1	Conclusion	105
	5.1.1 Objective 1	105
	5.1.2 Objective 2	105
	5.1.3 Objective 2	106
5.2	Recommendation	106
<b>REFERENCES</b>		<b>108</b>
<b>APPENDIX</b>		
<b>LIST OF PUBLICATIONS</b>		

## LIST OF TABLES

Table 3.1	Setup for simulation of one-dimensional dam break flow problem.	30
Table 3.2	Set up for mesh consistency test.	30
Table 3.3	Setup for simulation of two-dimensional partial dam break flow problem.	31
Table 3.4	Set up for verification of DA-CIP model against analytical solution.	34
Table 3.5	Set up for validation of numerical solution (DA-CIP and FLOW-3D model) against experimental results.	35
Table 3.6	Set up for physical experiment	50
Table 4.1	Comparison between analytical solution and simulation results	77

## LIST OF FIGURES

Figure 2.1	Designation of approach channel, tail water channel, $b_1$ is the width of approach channel and $b_2$ is the width of the tail water channel.	10
Figure 2.2	Flow features of supercritical flow at abrupt expansion structure.	11
Figure 2.3	Physical model of supercritical flow at abrupt expansion.	12
Figure 3.1	Research methodology.	18
Figure 3.2	Solution algorithm.	20
Figure 3.3	Designation of $u$ , $h$ in the staggered grid system employed in the one-dimensional DA-CIP model.	21
Figure 3.4	Designation of $u$ , $v$ , $h$ in the staggered grid system employed in the two-dimensional DA-CIP model.	24
Figure 3.5	Initial condition for the one-dimensional dam break scenario, with initial water depth of the reservoir at 2.0m.	29
Figure 3.6	Initial condition of the two-dimensional partial dam break problem.	32
Figure 3.7	Dimension of dam (plan view) for partial dam break problem.	32
Figure 3.8	Schematic of the abrupt expansion flow features.	33
Figure 3.9	Specification of the general properties under “General” tab.	36



Figure 3.10	Second step- “Physics” tab.	37
Figure 3.11	Set up of gravity component.	37
Figure 3.12	Set up of viscosity and turbulence component	38
Figure 3.13	Shallow water model is enabled in the model physics.	39
Figure 3.14	Set up of fluid properties.	40
Figure 3.15	Designation of “wall component” and “bed component”.	41
Figure 3.16	Set up for the geometry of the components.	41
Figure 3.17	Dimension of the components.	42
Figure 3.18	Overview of mesh system.	43
Figure 3.19	Position of “Mesh Block 1”.	44
Figure 3.20	Position of “Mesh Block 2”.	44
Figure 3.21	Grid information of “Mesh Block 1”.	45
Figure 3.22	Grid information of “Mesh Block 2”.	45
Figure 3.23	Inflow and outflow boundary conditions.	46
Figure 3.24	Wall boundary conditions.	47
Figure 3.25	Grid overlay conditions.	47
Figure 3.26	Experimental set up (upstream view).	48
Figure 3.27	Experimental set up (downstream view).	49
Figure 3.28	Test channel setup.	50
Figure 3.29	Supercritical flow at abrupt expansion channel.	51
Figure 3.30	Coefficient of discharge, $C_d$ according to British Standard.	53
Figure 3.31	Value of $k_b$ related to $b/B$ extracted from British Standard.	53

Figure 3.32	Outflow from rectangular weir.	54
Figure 3.33	Position at which velocity is measured.	55
Figure 3.34	Photo and illustrations of hot-film probe (a) side view (b) plan view (c) hot-film probe features (scaled up) (d) dimensions for the hot-film probe (in millimetres).	56
Figure 3.35	Modification at the inlet section.	57
Figure 3.36	Mesh system overlay on the channel bed.	58
Figure 4.1	The depth profile simulated with different cell sizes for one-dimensional dam break flow problem at (a) $t=0.10$ s (b) $t=0.30$ s (c) $t=0.50$ s.	60
Figure 4.2	The numerical and analytical solution for dam break flow over dry bed condition, at time $t=0.20$ s.	63
Figure 4.3	The numerical and analytical solution for dam break flow over dry bed condition, at time $t=0.40$ s.	63
Figure 4.4	The numerical and analytical solution for dam break flow over dry bed condition, at time $t=0.60$ s.	64
Figure 4.5	The numerical and analytical solution for dam break flow over dry bed condition, at time $t=0.80$ s.	64
Figure 4.6	The numerical and analytical solution for dam break flow over dry bed condition, at time $t=0.92$ s.	65
Figure 4.7	The numerical and analytical solution for dam break flow over dry bed condition, at time $t=1.00$ s.	65
Figure 4.8	The numerical and analytical solution for dam break flow over dry bed condition, at time $t=1.20$ s.	66

Figure 4.9	Flow profile at $t = 7.2$ s (from numerical simulation of DA-CIP) (a) perspective view and (b) flow depth contour.	67
Figure 4.10	Flow profile at $t = 7.2$ s (from Akoh et al. (2007) studies) (a) perspective view and (b) flow depth contour.	68
Figure 4.11	Simulated result for Case 1 ( $Fr = 2.0$ , plan view) at various time step.	70
Figure 4.12	Simulated result for Case 1 ( $Fr = 2.0$ , aerial view) at various time step.	71
Figure 4.13	Simulated result for Case 2 ( $Fr = 3.0$ , plan view) at various time step.	72
Figure 4.14	Simulated result for Case 2 ( $Fr = 3.0$ , aerial view) at various time step.	73
Figure 4.15	Simulated result for Case 3 ( $Fr = 4.0$ , plan view) at various time step.	74
Figure 4.16	Simulated result for Case 3 ( $Fr = 4.0$ , aerial view) at various time step.	75
Figure 4.17	Case 1: Simulation result for flow with $Fr = 2.0$ (plan view) and the comparison between analytical and numerical results	77
Figure 4.18	Case 2: Simulation result for flow with $Fr = 3.0$ (plan view) and the comparison between analytical and numerical results	78

Figure 4.19	Case 3: Simulation result for flow with $Fr = 4.0$ (plan view) and the comparison between analytical and numerical results	78
Figure 4.20	Simulated result for Case 4 ( $Fr = 2.45$ ) at various time step.	80
Figure 4.21	Simulated result for Case 5 ( $Fr = 2.50$ ) at various time step.	83
Figure 4.22	Flow profile along centreline of the channel for Case 4 ( $Fr = 2.45$ ).	87
Figure 4.23	Discrepancy ratio for Case 4 ( $Fr = 2.45$ ).	88
Figure 4.24	Discrepancy ratio for Case 4 ( $Fr = 2.45$ ).	88
Figure 4.25	Flow profile in transverse direction at $x=0.05\text{m}$ for Case 4 ( $Fr = 2.45$ ).	89
Figure 4.26	Flow profile in transverse direction at $x=0.10\text{m}$ for Case 4 ( $Fr = 2.45$ ).	90
Figure 4.27	Flow profile in transverse direction at $x=0.15\text{m}$ for Case 4 ( $Fr = 2.45$ ).	90
Figure 4.28	Flow profile in transverse direction at $x=0.20\text{m}$ for Case 4 ( $Fr = 2.45$ ).	91
Figure 4.29	Flow profile in transverse direction at $x=0.25\text{m}$ for Case 4 ( $Fr = 2.45$ ).	91
Figure 4.30	Flow profile in transverse direction at $x=0.30\text{m}$ for Case 4 ( $Fr = 2.45$ ).	92
Figure 4.31	Flow profile in transverse direction at $x=0.35\text{m}$ for Case 4 ( $Fr = 2.45$ ).	92

Figure 4.32	Flow profile in transverse direction at $x=0.40\text{m}$ for Case 4 ( $Fr = 2.45$ ).	93
Figure 4.33	Flow profile in transverse direction at $x=0.45\text{m}$ for Case 4 ( $Fr = 2.45$ ).	93
Figure 4.34	Flow profile in transverse direction at $x=0.50\text{m}$ for Case 4 ( $Fr = 2.45$ ).	94
Figure 4.35	Flow profile along centreline of the channel for Case 5 ( $Fr = 2.50$ ).	96
Figure 4.36	Discrepancy ratio for Case 5 ( $Fr = 2.50$ ).	97
Figure 4.37	Discrepancy ratio for Case 5 ( $Fr = 2.50$ ).	97
Figure 4.38	Flow profile in transverse direction at $x=0.05\text{m}$ for Case 5 ( $Fr = 2.50$ ).	98
Figure 4.39	Flow profile in transverse direction at $x=0.10\text{m}$ for Case 5 ( $Fr = 2.50$ ).	99
Figure 4.40	Flow profile in transverse direction at $x=0.15\text{m}$ for Case 5 ( $Fr = 2.50$ ).	99
Figure 4.41	Flow profile in transverse direction at $x=0.20\text{m}$ for Case 5 ( $Fr = 2.50$ ).	100
Figure 4.42	Flow profile in transverse direction at $x=0.25\text{m}$ for Case 5 ( $Fr = 2.50$ ).	100
Figure 4.43	Flow profile in transverse direction at $x=0.30\text{m}$ for Case 5 ( $Fr = 2.50$ ).	101
Figure 4.44	Flow profile in transverse direction at $x=0.35\text{m}$ for Case 5 ( $Fr = 2.50$ ).	101

Figure 4.45	Flow profile in transverse direction at $x=0.40\text{m}$ for Case 5 ( $Fr = 2.50$ ).	102
Figure 4.46	Flow profile in transverse direction at $x=0.45\text{m}$ for Case 5 ( $Fr = 2.50$ ).	102
Figure 4.47	Flow profile in transverse direction at $x=0.50\text{m}$ for Case 5 ( $Fr = 2.50$ ).	103

## LIST OF SYMBOLS

$b_1$	Width of the approach channel
$b_2$	Width of the tail water channel
$b_e$	Effective length [m]
$\beta$	Angle of shock wave
$C_d$	Effective coefficient of discharge
$C_0$	Speed of wave
$dt$	Time step interval [s]
$dx$	Cell size in x-direction
$dy$	Cell size in y-direction
$d_1$	Flow depth measured at sudden expansion
$Fr$	Froude number
$g$	Gravitational acceleration
$H_0$	Total head [m]
$h_0$	Approach depth / initial depth [m]
$h$	Flow depth [m]
$h^*$	Temporary values for water depth after calculation of advection phase with CIP scheme
$h_{le}$	Effective head measured above the weir crest [ft]
$n$	Manning's coefficient of roughness
$\theta$	Angle of flow expansion
$Q$	Flow discharge [m <sup>3</sup> /s]
$t$	Time [s]
$\tau$	Shear stress

$u$	Depth-averaged velocity in $x$ -direction
$u^*$	Temporary values for velocity after calculation of advection phase with CIP scheme in $x$ -direction
$\tilde{u}$	Second temporary values for velocity in $x$ -direction
$v_0$	Approach velocity
$v$	Depth-averaged velocity in $y$ -direction
$v^*$	Temporary values for velocity after calculation of advection phase with CIP scheme in $y$ -direction
$\tilde{v}$	Second temporary values for velocity in $y$ -direction
$\bar{V}$	Mean velocity of flow
$x$	Streamwise coordinate [m]
$y$	Transverse coordinate [m]



# **SIMULASI BERANGKA ALIRAN LAMPAU GENTING DI STRUKTUR PENGEMBANGAN MENDADAK DENGAN MODEL SKIM TARAF TINGGI**

## **ABSTRAK**

Dalam proses mereka bentuk struktur hidraulik, biasanya akan mengalami aliran lampau genting. Struktur pengembangan mendadak merupakan salah satu jenis struktur peralihan dalam struktur hidraulik buatan manusia, bertujuan untuk memenuhi perubahan geometri dalam saluran terbuka. Dalam membina struktur pengembangan mendadak, spesifikasi rekabentuk adalah penting untuk dipenuhi terutamanya apabila melibatkan aliran halaju tinggi. Penulis membina Model Kedalaman Purata Dua Dimensi (model DA-CIP) yang menggabungkan Skim Profil Interpolasi Terkawal (CIP) untuk meningkatkan ketepatan model berangka. Kajian ini menggunakan model DA-CIP yang disahkan dengan penyelesaian analitikal yang mensimulasikan masalah aliran empangan pecah. Seterusnya, penulis menggunakan model DA-CIP untuk mensimulasikan fenomena aliran lampau genting pada struktur pengembangan mendadak. Model DA-CIP mampu menghasilkan semula fenomena tersebut dengan ciri-ciri aliran seperti pembentukan garis penentuan, zon kedalaman dan halaju yang tetap dan gelombang bersilang di bahagian hiliran, serta mekanisme refleksi yang terbentuk di sisi dinding. Keputusan simulasi (tanpa tegasan ricih) disahkan dengan penyelesaian analitikal dan tahap kesepakatan yang berbeza dapat diperhatikan. Kajian ini membina model eksperimen fizikal yang menghasilkan aliran halaju tinggi pada saluran pengembangan mendadak bagi tujuan pengesahihan. Model DA-CIP menunjukkan nilai  $R^2$  setinggi 0.9702 untuk kes  $Fr = 2.45$  dan 0.9898 untuk kes  $Fr = 2.50$  dalam mensahkan dengan data eksperimen manakala nilai  $R^2$  yang agak rendah diperoleh apabila menggunakan model FLOW-3D.

# NUMERICAL SIMULATION OF SUPERCRITICAL FLOW AT ABRUPT EXPANSION STRUCTURE WITH HIGHER ORDER SCHEME

## ABSTRACT

In the design of hydraulic structures, it is common to deal with the supercritical flow. Abrupt expansion structure represents a type of transition often constructed in manmade hydraulic structure to cater the geometry difference. It is important to cater the design of such transition especially when it involves flow with high velocity. The author developed a two-dimensional depth-averaged model (DA-CIP model) incorporated with Constrained Interpolation Profile (CIP) scheme to increase the accuracy of the numerical model. This study tested the DA-CIP model with verification procedure against analytical solution of dam break flow problem. The author used the DA-CIP model to simulate the supercritical flow phenomena at abrupt expansion channel. The DA-CIP model was capable to reproduce the phenomena mentioned with the flow features such as the formation of demarcation line, zone of constant depth and velocity and the cross waves at the downstream, as well as the reflecting mechanism at the sidewall. The simulated results (without bottom shear stress) was verified with analytical solution and different degree of agreement was observed. This study developed a physical experimental model that reproduced the high-velocity flow at sudden expansion channel for validation purposes. The DA-CIP model shows a high  $R^2$  value of 0.9702 for case with  $Fr=2.45$  and 0.9898 for case with  $Fr =2.50$  when validated with experimental data while relatively low  $R^2$  value were obtained when using FLOW-3D model.

# CHAPTER ONE

## INTRODUCTION

### 1.1 Background

In the design of open channel, transition structure is widely used to allow lateral expansion or contraction of the flow. The effect on the flow due to sudden change in the geometry of open channel is commonly associated with supercritical flow. These high velocity flows often occur in man-made hydraulic structures such as chutes in dam structure, sewer in large drainage system or sometimes in channel for irrigation purposes. Supercritical flow possesses higher energy than subcritical flow, in which any abrupt changes in the flow direction involve high impact force and often accompanied by formation of shock wave and hydraulic jump. Such flow features can damage the hydraulic structure and the surrounding if the design of the transition is not handled properly. Therefore, in this study, understanding of such phenomenon is the principal subject.

Experience shows that a complicated model developed by a third party and calibrated by a consultant is a black-box. Black-box in the sense that user merely keys in the data, pressed the “run” button and model display result with no detailed understanding of modelling process. Therefore, we need to develop an in-house code which enable us to control its accuracy and highly flexible. It can be used to accurately simulate the phenomenon of supercritical flow at abrupt expansion structure.

The state of flow, whether it is supercritical or subcritical, is affected by gravity. It is represented by the ratio of inertial forces to gravity forces, known as Froude number. Whenever the Froude number of a flow is equal to unity, it is known

to be in critical flow state. If it is less than unity, the flow is subcritical, the flow depth is larger than the critical flow depth. If Froude number is greater than unity, the flow is supercritical, the flow depth is less than the critical flow depth. In supercritical flow state, the effect of inertial forces is more pronounced where the flow usually has high velocity (Chanson, 2004; Chow, 1959).

The pioneer studies on channel expansion was done by Rouse et al. (1951). The study discussed about the different surface profile for numerous Froude numbers and width-depth ratio. In Rouse et al. (1951) studies, the author concluded that the elementary wave theory is valid if the assumptions involved were approximately satisfied. A generalised diagram was presented for preliminary design of channel expansion.

By using a non-dimensional approach, Hager and Mazumder (1992) further investigate the axial and wall surface profiles and presented a generalised design method.. The study analysed the flow features in an abrupt expansion channel and the results may served as a basis for improving supercritical flow at abrupt expansion structure.

Hosoda and Yoneyama (1994) further expressed the relationships between Froude number and change in flow direction of supercritical flow through a different approach. These studies developed the analytical study for the abrupt channel flow, the angle of expansion and the angle formation of shock waves in which were derived based on method of characteristics.

In this study, the depth-averaged model (DA-CIP) was developed to simulate the supercritical flow ( $Fr > 1$ ) at the abrupt expansion structure. The depth-averaged model utilised these governing equations: the conservation of mass and conservation

of momentum. The advection phase in these equations was solved using Constrained Interpolation Profile (CIP) scheme which is a higher order scheme of third order accuracy.

Yabe et al. (1991) developed CIP scheme to solve the hyperbolic equation. The CIP method proposed are able to construct a solution inside the grid cell that is close to the real solution, with some constraints (Yabe et al., 2001b). These constraints such as time evolution of spatial gradient or spatially integrated conservative quantities are used to construct the profile (Yabe et al., 2001b). The CIP scheme is a robust and less diffusive solver and resulting in a solution of third order accuracy in space (Utsumi et al., 1997).

In this study, the author developed the DA-CIP model which can simulate the phenomenon of supercritical flow at abrupt expansion. The intention is to provide a better understanding towards this phenomenon and also aid in the design of such transition structure. Whereby, the model able to provide a prediction of the location of the flow features such as cross waves and flow depth near the impingement point at sidewall.

## **1.2 Problem Statement**

Abrupt expansion structure represents the transition in geometry of a hydraulic structure. When dealing with the supercritical flow at the abrupt expansion, the design of this transition structure must be properly carried out. Whenever the transition is too rapid or abrupt, it causes a major part of the supercritical flow fail to be confined within the boundaries. If the divergence is too gradual, it results in a waste of material (over design). If local disturbances of excessive wave height are produced by improper boundary geometry, the walls may fail to confine the flow.

Therefore, satisfactory design of the expansion channel is crucial. Numerical simulation could act as a modelling tool to simulate the flow at sudden expansion to determine the optimum design.

Proprietary software such as Flow3D, Fluent, Solidworks are common modelling tools involve in the simulation of water and environmental related phenomena. However, these software may introduce high license fee which in turn make up a larger part in the total system cost when considering hardware and software. The effect of high software license fees is more prominent in developing countries, in which research showed that proprietary software is not favourable in these countries in general (Paudel et al., 2010). Hence, these simulations require an alternatively low-cost modelling tool. Furthermore, computational models might come in handy when dealing with conditions that are difficult to reproduce in the laboratories.

### **1.3 Objectives**

The objectives of this study are:

- To develop a two-dimensional depth-averaged model (DA-CIP) which can simulate the phenomenon of supercritical flow at the abrupt expansion structure and the cross waves forming at the downstream of the flow;
- To improve the accuracy of the numerical model by incorporating a third order numerical scheme, Constrained Interpolation Profile (CIP); and
- To investigate and further clarify the flow characteristics of supercritical flow at abrupt expansion structure.

## **1.4 Scopes of Work**

The current research focuses on the development of a numerical model which can reproduce the flow structures and velocities at abrupt expansion structure with high accuracies. The numerical model is developed using the FORTRAN programming language. With the adoption of higher order numerical scheme through CIP, the order of accuracy of the numerical model is increased. The developed model is verified against benchmarking on phenomenon namely the one-dimensional dam break problem and two-dimensional partial dam break problem. The numerical model is then validated against experimental data obtained from a physical model constructed in the Hydraulic Laboratory of River Engineering and Urban Drainage Research Centre (REDAC). An abrupt expansion channel was constructed for conducting the experiments, the supercritical flow condition is engaged along with in order to produce such phenomenon mentioned. Due to the limitation of the laboratory pump system, the Froude number applied to the inflow is between 2.45 and 2.50. In this study, another numerical model is also developed using FLOW-3D, a proprietary software. The FLOW-3D model is developed using the same condition specified in the physical experimental setup.

## **1.5 Organisation of the Thesis**

This thesis is divided into five chapters. Chapter One describes the brief introduction and discussion on the supercritical flow in abrupt expansion channel along with objectives and scopes of this study. In this chapter, a brief discussion about the state of flow, numerical model and its adoption of CIP scheme is also included.

Chapter Two addresses several topics about supercritical flow in abrupt expansion channel, such as the mechanics of supercritical flow, state of flow and

flow characteristics. This chapter also outlines a literature review of earlier works and developments regarding supercritical flow experiments and its analytical studies. Furthermore, the chapter also reviews the development of CIP scheme that adopted in the numerical model, DA-CIP.

Chapter Three discusses the research method employed to achieve the objectives of this study. The development of the numerical model, DA-CIP, and its numerical algorithm along with the verification and validation procedures are elaborated in this chapter. The experimental works and its working procedures are also discussed in this chapter.

Chapter Four presents the research outcomes of this study. These include the results from verification process between the numerical model, DA-CIP, and analytical model. The outcomes aid in developing a suitable model that can simulate the supercritical flow at abrupt expansion phenomena. The outcomes of validation process between simulated and experimental results are also presented in this chapter.

Chapter Five summarises and concludes the outcomes of this study along with the recommendations for future work.



## CHAPTER TWO

### LITERATURE REVIEW

#### 2.1 Overview

Supercritical flow refers to a state of flow whereby the inertial forces are more dominance than gravitational force. The state of flow is discussed in Section 2.2. Section 2.3 discusses the mechanism behind supercritical flow and the reason this study focuses on this state of flow. Section 2.4 explains the background of supercritical flow in abrupt expansion, and subsequently the pioneer experimental work is described in Section 2.5. The flow characteristics of supercritical flow at abrupt expansion channel is presented in Section 2.6, while the analytical study is showed in Section 2.7. Section 2.8 describes the background of Constrained Interpolation Profile (CIP) scheme.

#### 2.2 State of Flow

The behaviour of open channel flow is governed by the effect of gravity and inertial forces of the flow. Since the flow in most channel is controlled by the gravity effect, the ratio of inertial forces to gravity forces is more suitable to describe the state of flow (Chow, 1959; Radecki-Pawlik et al., 2017). Such ratio is named as Froude number,  $Fr$ , that is defined as

$$Fr = \frac{\bar{V}}{\sqrt{gL}} \quad (2.1)$$

where  $\bar{V}$  is the mean velocity of flow,  $g$  is the gravitational acceleration and  $L$  is the characteristic length. In open channel flow, the parameter of characteristic length,  $L$  is equal to the hydraulic depth. Hydraulic depth is defined as the cross-section area of

the flow divided by the width of the free surface. For rectangular channel, this is equal to the depth of flow,  $D$  (Chow, 1959; Radecki-Pawlik et al., 2017).

Therefore, Eq. 2.1 gives

$$Fr = \frac{\bar{V}}{\sqrt{gD}} \quad (2.2)$$

When  $Fr$  is equal to one, the flow is defined as critical flow. If  $Fr$  is less than one, then the flow is subcritical. A state of flow is said to be supercritical when  $Fr$  is greater than one, in which this state the inertial forces is more dominance than the gravitational forces (Chow, 1959; Radecki-Pawlik et al., 2017) and therefore the gravitational effects can be neglected.

### **2.3 Mechanics of Supercritical Flow**

For decades, problems involving high-velocity flow at open channel transition were generally solved by physical model test. However, researchers realised that general principles of such phenomenon must be addressed. With such principles, simple designs can be made without the need of obtaining empirical solution from experiment to allow complex designs to be approximated before experimental refinement (Ippen, 1951). Due to the deficiency in technical literature, Ippen (1951) presented a comprehensive theory of high velocity flow in the High-Velocity flow in Open Channels symposium in 1951.

Ippen (1951) demonstrated the characteristics of supercritical flow by referring to the specific head concept. In the case of supercritical flow ( $Fr > 1$ ), velocity head commonly exceeded the depth in order of magnitude. in addition, enormous differences in specific head are accompany with large variations in velocity head. Although small variations in the boundaries contribute to relatively

small pressure in terms of velocity head, the changes in surface elevation were relatively large.

#### **2.4 Expansion in Supercritical Flow**

A pioneer study on channel expansion was done by Rouse et al. (1951). The study discussed about the different surface profiles for numerous Froude numbers and width-depth ratios.

The channel expansion problem which involved supercritical flow can be solved using analytical approach, provided that

- the channel walls were vertical;
- the channel bed was horizontal;
- the energy loss due to boundary resistance was negligible; and
- the pressure was assumed hydrostatic pressure.

(Chow, 1959; Rouse et al., 1951)

The results could be presented in the generalized diagram form for convenient in preliminary design. Rouse et al. (1951) concluded that the results from the experiment of supercritical flow in open channel expansion showed a close agreement with the elementary wave theory if the assumptions involved (mentioned above) were satisfied.

A quasi-2D calculation model was developed and studies by Amara, Berreksi and Achour (2017) for applications to steady supercritical flow in abrupt channel expansion. By transforming the two-dimensional space-dependent problem to one-dimensional time-dependent problem, an asymptotic solution was derived. The model performed well despite there is some limitations in the depth-averaged equation especially in vicinity of strong shock front.

## 2.5 Abrupt Expansion Experimental Study

Hager and Mazumder (1992) analysed the phenomenon of abrupt expansion channel under supercritical flow condition using a semi empirical approach. Series of experiment were carried out and the flow features in abrupt channel expansion such as the formation of shock front, expansion of flow region and the flow reflection mechanism at the wall were described. The study showed that both the axial and transverse profiles were independent of the expansion ratio ( $b_2/b_1$ ) between the approach channel and tail water channel. Fig. 2.1 shows the approach channel and tail water channel described by Hager and Mazumder (1992).

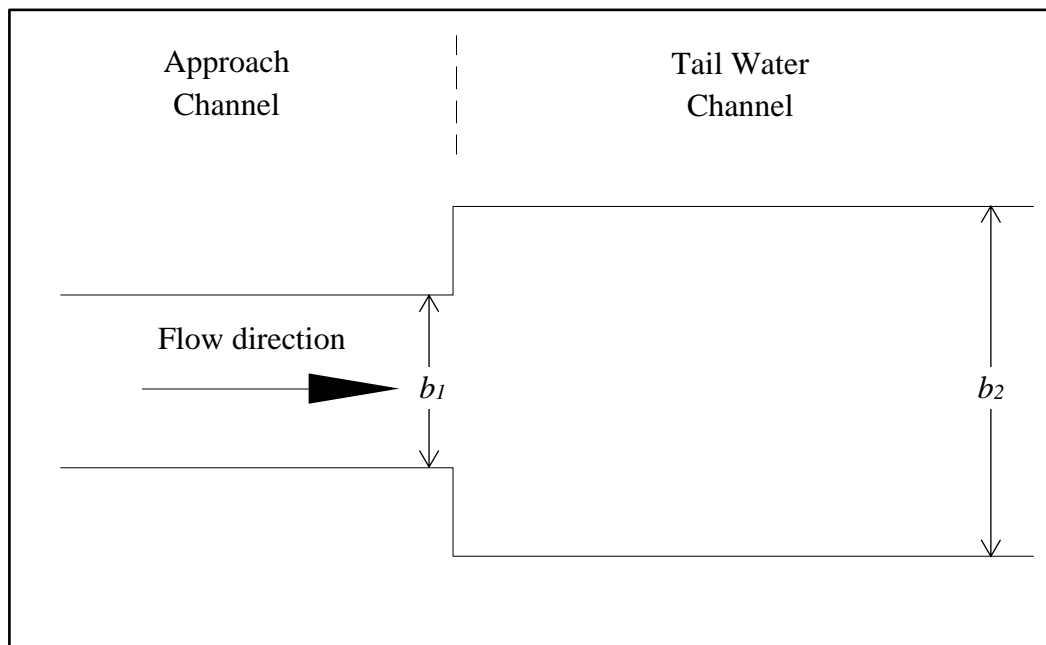


Figure 2.1: Designation of approach channel, tail water channel,  $b_1$  is the width of approach channel and  $b_2$  is the width of the tail water channel (Hager & Mazumder, 1992).

## 2.6 Flow Characteristics of Supercritical Flow at Abrupt Expansion Channel

In the case of supercritical flow occurring at the abrupt expansion transition, the flow emerging from the expansion was subjected to change in direction at an angle  $\theta$ , which was referred to as the angle of flow expansion as shown in Fig. 2.2. The flow then impinges at the side wall of the tail water channel i.e. the impingement points,

forming oblique standing waves at an angle  $\beta$  which was referred to as the angle of shock wave (Fig. 2.2). These oblique standing waves continued undiminished towards the centre of the channel, in the downstream direction before crashing into each other at the centre of the channel (Ippen, 1951).

There was a region at the abrupt expansion where the flow depth and velocity were constant and equivalent to the approach flow depth,  $h_0$  and approach velocity,  $V_0$ . This triangular region was known as the zone of constant depth and velocity (Hosoda & Yoneyama, 1994).

Fig. 2.3 shows the physical experiment set up in Kyoto University to reproduce the flow features of Supercritical flow at abrupt expansion channel (Puay, 2010). This study provides a guideline for the author to identify the important flow features when running the physical experiment.

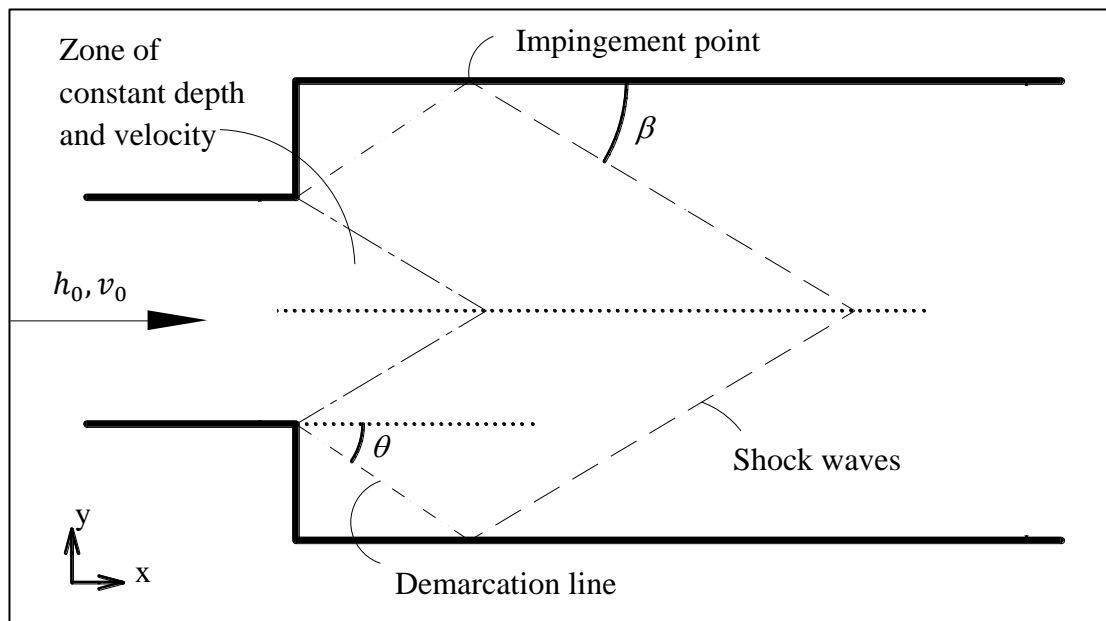


Figure 2.2: Flow features of supercritical flow at abrupt expansion structure (Hosoda & Yoneyama, 1994).



Figure 2.3: Physical model of supercritical flow at abrupt expansion (Puay, 2010).

## 2.7 Analytical Study

By using the governing equations, Ippen (1951) derived a unique relation between total head at the upstream before flow expansion with the velocity magnitude and flow direction at an arbitrary point in the flow expansion zone as follows,

$$H_0 = \frac{V^2}{2g} + h_0 = \text{constant} \quad (2.3)$$

$$\frac{1}{V} \frac{dV}{d\theta} = \frac{\sqrt{H_0 - \frac{V^2}{2g}}}{\sqrt{\frac{3V^2}{2g} - H_0}} \quad (2.4)$$

where  $V$  is defined as  $V \equiv \sqrt{u^2 + v^2}$  and  $\theta$  is  $\tan \theta = \frac{v}{u}$

Eq. 2.3 is true in the domain before any shock wave or jump occurs.

By introducing  $V' = \frac{V}{\sqrt{2gH_0}}$ , the dimensionless form of Eq. 2.3 and Eq. 2.4 can be

expressed as follows:

$$V'^2 + \frac{h}{H_0} = 1 \quad (2.5)$$

$$\frac{1}{V'} \frac{dV'}{d\theta} = \frac{\sqrt{1 - V'^2}}{\sqrt{3V'^2 - 1}} \quad (2.6)$$

By integrating Eq. 2.6, the solution of  $\theta$  can be derived as follow:

$$\theta = \sqrt{3} \tan^{-1} \sqrt{\frac{\frac{3h}{2H_0}}{\left(1 - \frac{3h}{2H_0}\right)}} - \tan^{-1} \left( \frac{1}{\sqrt{3}} \right) \sqrt{\frac{\frac{3h}{2H_0}}{\left(1 - \frac{3h}{2H_0}\right)}} - \theta_1 \quad (2.7)$$

where  $\theta_1$  constitutes the integral constant specified by the condition that for  $\theta=0$ , the depth,  $h$  is the initial depth,  $h_0$  (i.e.  $h = h_0$ ). Angle  $\theta$  is referred to angle of flow expansion.

Also, Eq. 2.7 can be described in an alternate form using the Froude number:

$$\theta = \sqrt{3} \tan^{-1} \frac{\sqrt{3}}{\sqrt{Fr^2 - 1}} - \tan^{-1} \frac{1}{\sqrt{Fr^2 - 1}} - \theta_1 \quad (2.8)$$

It is worth to note that the solution in Eq. 2.7 and Eq. 2.8 are valid under the following maximum and minimum threshold conditions:

$$V' = 1 \quad \theta = 0^\circ \quad h/H_0 = 0 \quad (2.9)$$

$$V' = 1/\sqrt{3} \quad \theta = 65^\circ 53' \quad h/H_0 = 2/3 \quad (2.10)$$

In the case where the depth difference across the shock wave is small, the angle of shock wave,  $\beta$  is given in simplified form (Ippen, 1951):

$$\sin \beta = \frac{1}{Fr} \quad (2.11)$$

The analytical solution developed by Ippen (1951) is still commonly referred during desk studies despite its been published years back due to its comprehensive and accurate study, this can be seen in various studies such as (De Padova et al., 2013; Kochanenko et al., 2016; Mignot et al., 2016; Nanía et al., 2014; Riviere et al., 2017)

## **2.8 Constrained Interpolation Profile (CIP) Scheme**

The Constrained Interpolation Profile (CIP) was developed by (Yabe, 1991) to solve the hyperbolic equation. CIP scheme can be considered as a kind of semi-Lagrangian method, where a Lagrangian invariant solution was employed by CIP scheme. The Lagrangian invariant solution used was based on spatial points and was always casted in a non-conservative form (Yabe et al., 2001a). Semi-Lagrangian method that traced back along the characteristics in time depended on an interpolation of the initial profile to determine the value at the upstream departure point (Yabe et al., 2001b). The CIP method proposed here allowed the construct of a solution inside the grid cell that was close to the real solution, with some constraints (Yabe et al., 2001b). These constraints such as time evolution of spatial gradient or spatially integrated conservative quantities were used to construct the interpolation profile (Yabe et al., 2001b). Since adaptive grid system was not required in CIP method, the problems of grid distortion caused by structural breakup and topology change can therefore be eliminated (Yabe et al., 2001b). The CIP scheme was a robust and less diffusive solver, resulting in a solution of third order accuracy in space (Utsumi et al., 1997).

## **2.9 FLOW-3D model**

FLOW-3D is one of the widely used Computational Fluid Dynamics (CFD) commercial software, especially in solving three-dimensional flows phenomenon and are well known for its strength in free surface flow analysis (Brown & Crookston, 2016; Taghavi & Ghodousi, 2016; Taghavi & Ghodousi, 2015).

From Taghavi and Ghodousi (2015) study, FLOW-3D is more user friendly compared to the other CFD software. The software provide an easy way in



developing the solid boundaries and mesh system as well as automatic selection of the optimum time step during simulation. The computations using FLOW-3D are based on orthogonal rectangular grid system in which is it a more easy way to generate and compute (Gabl et al., 2015).

## **2.10 Dam Break Flow Problem**

In order to investigate the performances of the numerical model, an idealised scenario of dam break flow problem in a rectangular channel is simulated. Ji et al. (2013) mentioned that the dam break flow problem is a widely used benchmarking problem in investigating the accuracy and stability of the numerical model. The wide acceptance of the dam break flow problem as a verification test can be seen in previous research (Caleffi et al., 2003; He et al., 2018; Ji et al., 2013; Ozmen-cagatay & Kocaman, 2010; Schippa & Pavan, 2011; Yang et al., 2010).

For instance, Liu et al. (2017) presented a two-dimensional, two-phase debris flow numerical model based on finite volume method. The validation part was carried out against one-dimensional and two-dimensional dam break flow problem before the model was applied on two-phase debris flow problem.

Caleffi et al. (2003) presented a two-dimensional shallow water model by finite volume method based on Godunov approach. The paper presented a few verification methods including one-dimensional steady flow with shock over bump, two-dimensional oblique hydraulic jump, and the inclusion of two-dimensional partial dam break flow problem over wet bed and dry bed. After obtaining a good result in verification, the simulation of a flood event on the Toce River valley was then carried out with the numerical model developed.

On the other hand, He et al., (2018) proposed a Smoothed Particle Hydrodynamics and Discrete Element Method (SPH-DEM) model to simulate the particle-fluid flow with free surface. In this study, the dam break flow problem was utilised to verify his SPH-DEM model.

Researcher often test the accuracy of their numerical model with dam break flow problem before it was applied to the phenomenon addressed. The dam break flow problem includes a largely distorted free surface which allows the study of the capability of the numerical model to reproduce the discontinuous solution (Caleffi et al., 2003; Ji et al., 2013). Furthermore, the simplicity in setting up the initial and boundary conditions makes the verification process more straightforward for free surface flow. (He et al., 2018; Ji et al., 2013).

### **2.11 Discrepancy Ratio**

Discrepancy ratio represents the ratio between predicted value and observed value (Bong et al., 2016; Gaucher et al., 2010). This ratio is used when comparing the numerical results and experimental results in validation of the model.

$$Discrepancy\ Ratio = \frac{Predicted\ value}{Observed\ value} \quad (2.12)$$

### **2.12 Summary**

This chapter discusses the characterisation of state of flow and the mechanics of supercritical flow. The literature studies of supercritical flow at sudden expansion channel have provided the basis of setting up the computational model as well as the physical model developed for this study. The Constrained Interpolation Profile (CIP) scheme will be incorporated in the development of depth-averaged model (DA-CIP).

## **CHAPTER THREE**

### **METHODOLOGY**

#### **3.1 Introduction**

This chapter discusses the research methodology employed in this study. The research methodology flow chart is presented in Fig. 3.1. The development of the one-dimensional and two-dimensional DA-CIP model is explained in Section 3.2. The model will undergo verification procedures against benchmarking problem and also tested for its mesh consistency. Section 3.3 elaborates the simulation of supercritical flow at abrupt expansion channel using the verified DA-CIP model. In this section, the verification and validation measures also will be presented. The development of FLOW-3D model is discussed in Section 3.4. While Section 3.5 explains the development physical model.

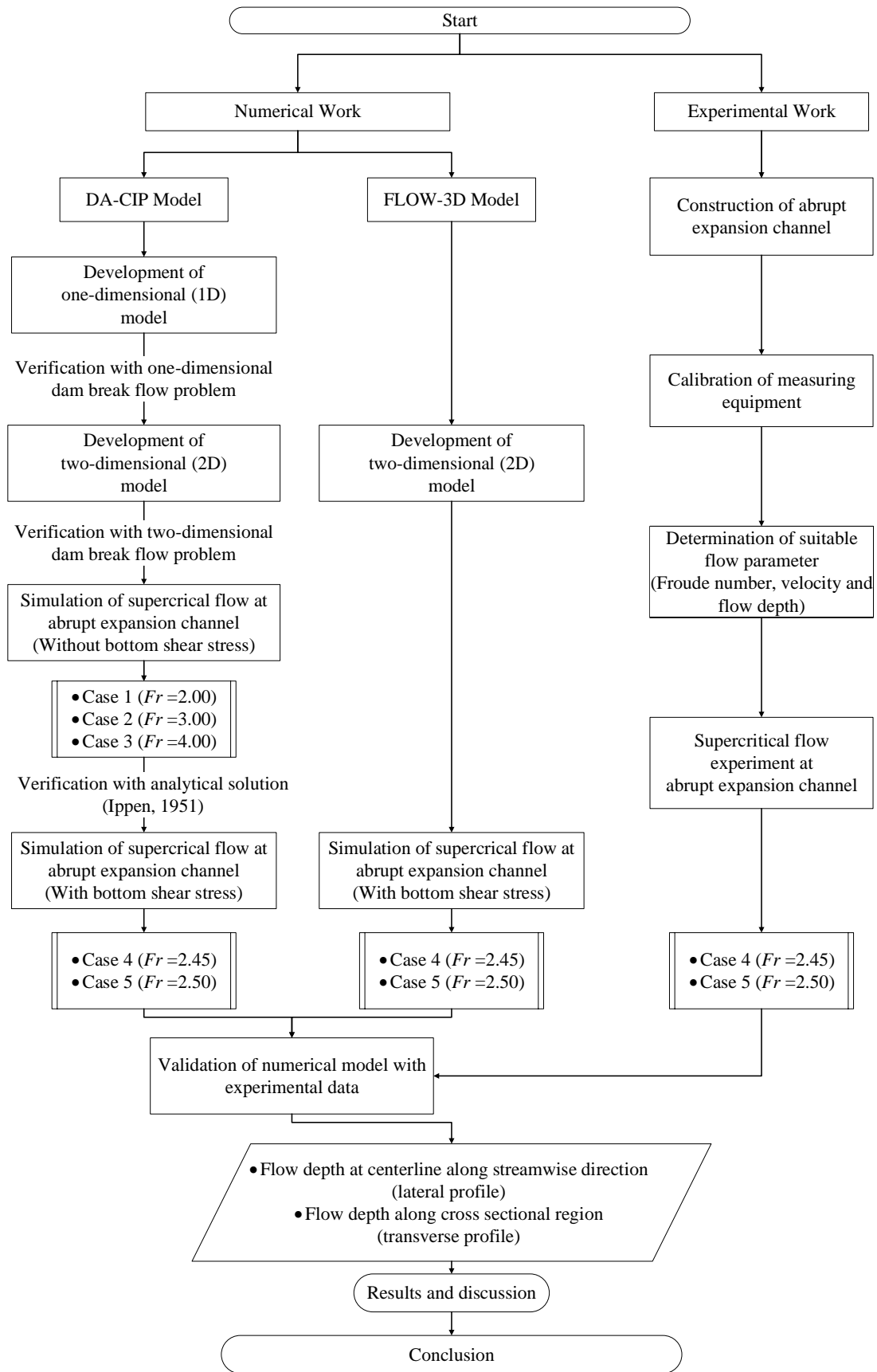


Figure 3.1: Research methodology.

### 3.2 Development of Numerical Model (DA-CIP)

The one-dimensional DA-CIP model is developed based on the one-dimensional non-conservative form of continuity and momentum equation. The developed model is tested for its accuracy by verifying it with the analytical solution i.e. Ritter's solution (Chanson, 2004). The one-dimensional model is then extended into two-dimensional form and verified with a two-dimensional partial dam break flow problem and compared with previous literature study's result (Akoh, 2007).

The two-dimensional DA-CIP model is then used to simulate the high-velocity flow at abrupt expansion channel without bottom shear stress. This model is then verified with the analytical solution developed by Ippen (1951).

Then, the DA-CIP is used to simulate the supercritical flow at sudden expansion channel with bottom shear stress in order to validate it with the physical experiment. In order to answer the problem statement, a similar numerical setup is carried out with FLOW-3D model, and comparison with DA-CIP model and physical model is made.

The numerical algorithm is summarised in Fig. 3.2, which in the case of one-dimensional problem, the depth-averaged velocity only considered the  $x$ -component ( $u$ ). In two-dimensional problem, both the  $x$  and  $y$  component of depth-averaged velocity ( $u, v$ ) is considered.

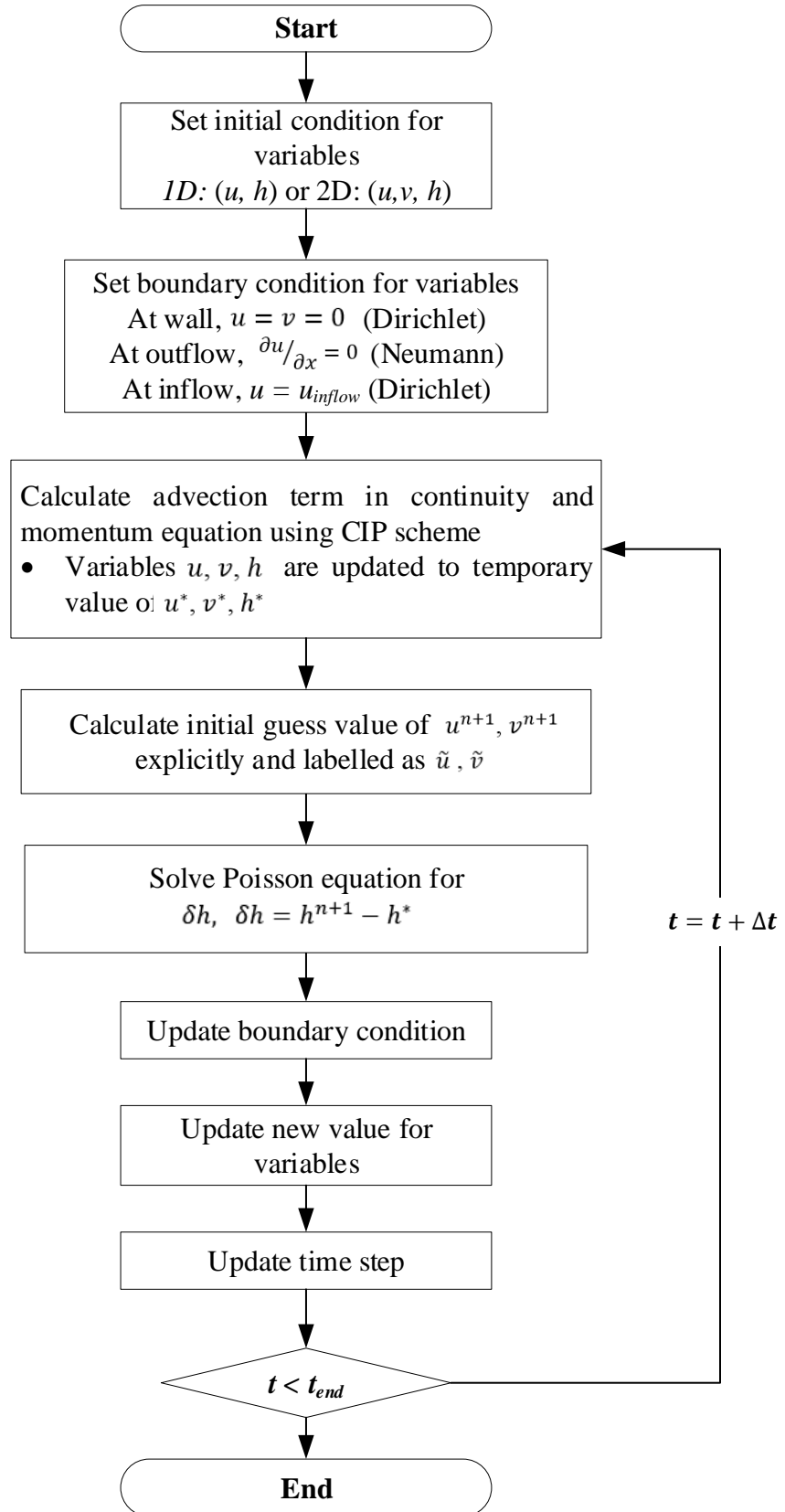


Figure 3.2: Solution algorithm.

### 3.2.1 Numerical Algorithm (One-dimensional problem)

The governing equations of the numerical model consist of the one-dimensional depth-averaged continuity and momentum equations as such,

Continuity Equation:

$$\frac{\partial h}{\partial t} + u \frac{\partial h}{\partial x} = -h \frac{\partial u}{\partial x} \quad (3.1)$$

Momentum Equation:

$$\frac{\partial u}{\partial t} + u \frac{\partial u}{\partial x} = -g \frac{\partial h}{\partial x} - gn^2 \frac{u|u|}{h^{\frac{4}{3}}} \quad (3.2)$$

Here,  $u$  is the depth averaged velocity,  $h$  is the depth of flow,  $n$  is Manning's coefficient of roughness, and  $g$  is the gravitational acceleration.

The governing equations are solved in two steps using the time-splitting method (Yabe et al., 2001a). In the first step, the advection terms in the continuity and momentum equations are solved using the CIP scheme.

The governing equations are discretized using the Finite Difference Method (FDM) (Anderson et al., 2012). The variables  $u$ , and  $h$  are defined in the grid system as shown in Fig. 3.3 based on the staggered grid system.

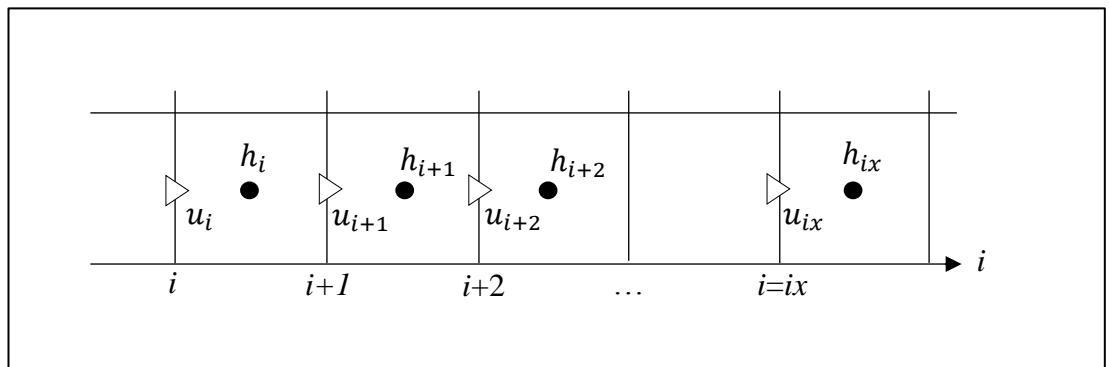


Figure 3.3: Designation of  $u, h$  in the staggered grid system employed in the one-dimensional DA-CIP model.

The numerical algorithm for one-dimensional case is as follow:

**Step one:**

The initial conditions and boundary conditions for different cases are setup. Then, the advection terms in the continuity and momentum equations are solved using the CIP scheme using the initial value:  $h^n$  and  $u^n$ . The new values after the solution of the advection term with CIP are then stored as  $h^*$  and  $u^*$ .

Continuity Equation (Advection terms):

$$\frac{\partial h}{\partial t} + u \frac{\partial h}{\partial x} = 0 \quad \longrightarrow \quad h^n \xrightarrow{CIP} h^* \quad (3.3)$$

Momentum Equation (Advection terms):

$$\frac{\partial u}{\partial t} + u \frac{\partial u}{\partial x} = 0 \quad \longrightarrow \quad u^n \xrightarrow{CIP} u^* \quad (3.4)$$

**Step two:**

The non-advection terms in the continuity and momentum equation is solved using the Finite Difference Method (FDM) and discretised based on the staggered grid system (Fig. 3.3).

Continuity Equation (Non-advection terms):

$$\frac{\partial h}{\partial t} = -h \frac{\partial u}{\partial x} \quad \longrightarrow \quad \frac{h_i^{n+1} - h_i^*}{\Delta t} = -h^* \left( \frac{\partial u}{\partial x} \right)_i^{n+1} \quad (3.5)$$

Momentum Equation (Non-advection terms)

$$\frac{\partial u}{\partial t} = -g \frac{\partial h}{\partial x} \quad \longrightarrow \quad \frac{u_i^{n+1} - u_i^*}{\Delta t} = -g \left( \frac{\partial h}{\partial x} \right)_i^{n+1} \quad (3.6)$$

Based on Eq. 3.6, an initial guess value  $\tilde{u}$  can be established as follows,

$$\frac{\tilde{u}_i - u_i^*}{\Delta t} = -g \left( \frac{\partial h}{\partial x} \right)_i^* \quad (3.7)$$

Subtracting Eq. 3.7 from Eq. 3.6 yields,

$$\frac{u_i^{n+1} - \tilde{u}_i}{\Delta t} = -g \left[ \left( \frac{\partial h}{\partial x} \right)_i^{n+1} - \left( \frac{\partial h}{\partial x} \right)_i^* \right] = -g \frac{\partial}{\partial x} (\delta h_i) \quad (3.8)$$



Where, 
$$\delta h_i = h_i^{n+1} - h_i^* \quad (3.9)$$

Therefore, from Eq. 3.8.

$$u_i^{n+1} = \tilde{u}_i - g\Delta t \frac{\partial}{\partial x}(\delta h_i) \quad (3.10)$$

Differentiating Eq. 3.10 with respect to  $x$  yields,

$$\frac{\partial u_i^{n+1}}{\partial x} = \frac{\partial \tilde{u}_i}{\partial x} - g\Delta t \frac{\partial^2}{\partial x^2}(\delta h_i) \quad (3.11)$$

By substituting Eq. 3.11 into Eq. 3.5, the following Poisson equations can be derived.

$$\frac{\delta h_i}{\Delta t} = -h^* \left[ \left( \frac{\partial \tilde{u}}{\partial x} \right)_i - g\Delta t \frac{\partial^2}{\partial x^2}(\delta h_i) \right] \quad (3.12)$$

$$\frac{\partial^2(\delta h_i)}{\partial x^2} = \frac{1}{g\Delta t} \left( \frac{\delta h_i}{\Delta t h^*} + \frac{\partial u^*}{\partial x} \right) \quad (3.13)$$

The Poisson equation in Eq. 3.13 is solved with Successive Over Relaxation (SOR) method for  $\delta h$ .

**Step three:**

The new value at the next time step,  $h^{n+1}$  and  $u^{n+1}$  can be updated based on Eq. 3.9 and Eq. 3.10 as follows,

$$h_i^{n+1} = h_i^* + \delta h_i \quad (3.14)$$

$$u_i^{n+1} = \tilde{u}_i - g\Delta t \frac{\partial}{\partial x}(\delta h_i) \quad (3.15)$$

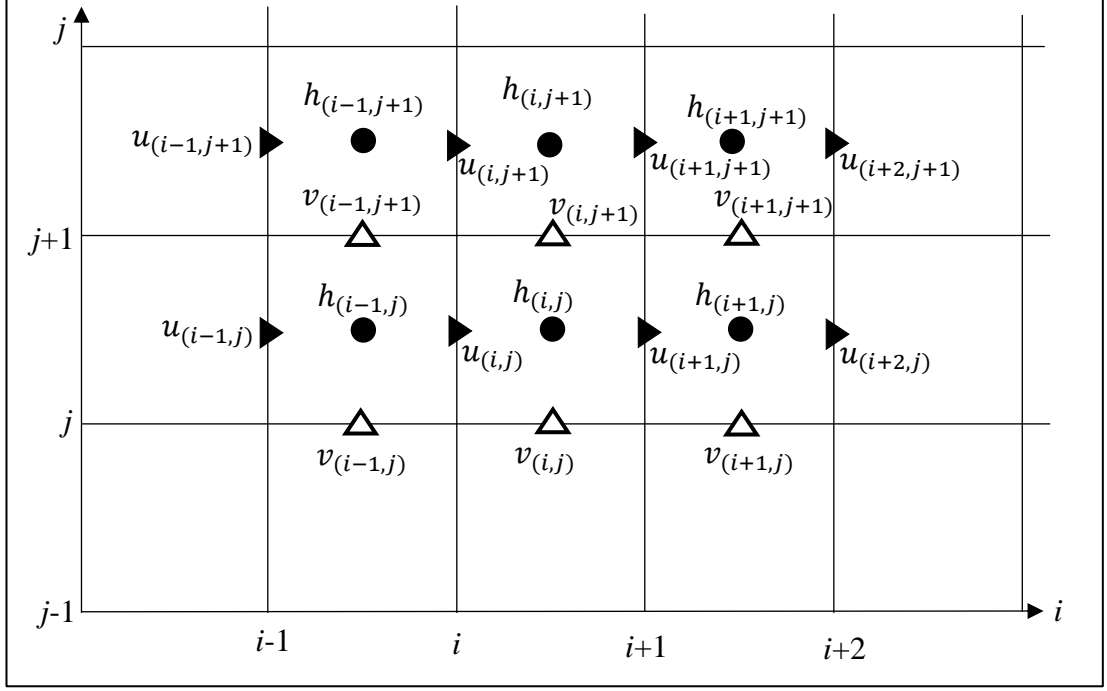


Figure 3.4: Designation of  $u$ ,  $v$ ,  $h$  in the staggered grid system employed in the two-dimensional DA-CIP model.

### 3.2.2 Numerical Algorithm (Two-dimensional Problem)

The two-dimensional depth-averaged model (DA model) is developed based on the following governing equation in their non-conservative form.

Continuity Equation:

$$\frac{\partial h}{\partial t} + u \frac{\partial h}{\partial x} + v \frac{\partial h}{\partial y} = -h \left( \frac{\partial u}{\partial x} + \frac{\partial v}{\partial y} \right) \quad (3.16)$$

Momentum Equation:

$$\frac{\partial u}{\partial t} + u \frac{\partial u}{\partial x} + v \frac{\partial u}{\partial y} \quad (3.17)$$

$$= -g \left( \frac{\partial h}{\partial x} + \frac{\partial z_b}{\partial x} \right) - \frac{gn^2 u \sqrt{u^2 + v^2}}{h^{1/3}} + \frac{\partial}{\partial x} \left( -\overline{u'^2 h} \right) + \frac{\partial}{\partial y} \left( -\overline{u'v' h} \right)$$

$$\frac{\partial v}{\partial t} + u \frac{\partial v}{\partial x} + v \frac{\partial v}{\partial y} \quad (3.18)$$

$$= -g \left( \frac{\partial h}{\partial y} + \frac{\partial z_b}{\partial y} \right) - \frac{gn^2 v \sqrt{u^2 + v^2}}{h^{1/3}} + \frac{\partial}{\partial x} \left( -\overline{u'v' h} \right) + \frac{\partial}{\partial y} \left( -\overline{v'^2 h} \right)$$